J|A|C|S
ARTICLES
Published on Web 06/06/2006

Investigation of Dipolar-Mediated Water−Protein Interactions in Microcrystalline Crh by Solid-State NMR Spectroscopy

Anne Lesage,*,‡ Lyndon Emsley,‡ François Penin,§ and Anja Böckmann*,§

Contribution from the Laboratoire de Chimie (UMR 5182 ENS/CNRS), Ecole Normale Supérieure de Lyon, 46 Allée d'Italie, 69364 Lyon, France, and Institut de Biologie et Chimie des Protéines, UMR 5086 CNRS/UCBL, IFR128 BioSciences Lyon-Gerland, 7, passage du Vercors, 69367 Lyon, France

Received February 6, 2006; E-mail: anne.lesage@ens-lyon.fr; a.bockmann@ibcp.fr

Abstract: Water−protein interactions play a major role in protein folding, structure, and function, and solid-state NMR has recently been shown to be a powerful tool for the site-resolved observation of these interactions in solid proteins. In this article we report investigations on possible water−protein dipolar transfer mechanisms in the microcrystalline deuterated protein Crh by a set of solid-state NMR techniques. Double-quantum (DQ) filtered and edited heteronuclear correlation experiments are used to follow direct dipolar water−protein magnetization transfers. Experimental data reveal no evidence for "solid-like" water molecules, indicating that residence times of solvent molecules are shorter than required for DQ creation, typically a few hundred microseconds. An alternative magnetization pathway, intermolecular cross-relaxation via heteronuclear nuclear Overhauser effects (NOEs), is probed by saturation transfer experiments. The significant additional enhancements observed when irradiating at the water frequency can possibly be attributed to direct heteronuclear water−protein NOEs; however, a contribution from relayed magnetization transfer via chemical exchange or proton−proton dipolar mechanisms cannot be excluded.

1. Introduction

Water is the unique environment to whose physical properties evolution adapted the molecular machinery of life. Protein−water interactions play an essential role in folding, structure, and stability of proteins, as well as in ligand binding, recognition, and catalysis. Nuclear relaxation was recognized early on as an important means to study protein hydration in solution via two complementary NMR techniques: (i) one using magnetic relaxation dispersion (MRD) of the quadrupolar ^{2}H and ^{17}O nuclei of water molecules,[1] which looks at the interactions via the solvent magnetization, and (ii) one using proton−proton nuclear Overhauser effects (NOE),[2] which reports these interactions on the protein spins in a site-resolved manner. The relevant pathways of magnetization transfer between water and proteins have been subjected to extensive studies (see, for example, refs 1−3). They include chemical exchange via labile protein protons and intermolecular $^{1}H-^{1}H$ dipolar cross-relaxation via internal or external water molecules. Although protein hydration has been studied for over a century, "progress has been slow and erratic".[1] Only very recently did a unifying picture of water dynamics on the surface of biological systems in solution emerge.[4] In particular, Halle, Otting, and co-workers found that, in the absence of chemical exchange, observed intermolecular NOEs are in most cases dominated by long-range dipolar couplings to bulk water. This allowed the conclusion that the diffusion of hydration water molecules at the surface of proteins in solution appears to be only marginally retarded as compared to that in bulk water.[4,5] If present, only water molecules in fully or partly buried hydration sites show longer residence times (up to the millisecond time scale). Chemical exchange between labile protein protons and water molecules has been for a long time disregarded as a possible magnetization transfer pathway competing with cross-relaxation. Biased interpretations resulted from this neglect,[6] which has been identified as a major source of misinterpretation of water−protein interactions in the past.[1,7,8]

Nevertheless, chemical exchange with water has been extensively studied for proteins in solution over a wide range of temperatures, pH, and concentration.[8] In particular, physiological conditions are of central interest as to the importance of water−protein magnetization transfer in magnetic resonance imaging (MRI). In this context, it has been shown that, in solutions at pH 7 and 36 °C,[8] as well as for the mobile components in cells in vitro and in vivo,[3] water−protein magnetization transfer is dominated by chemical exchange of fast-exchanging hydroxyl or amino protons.

Though many studies on water−protein interactions have been performed in solution, there are to date only a few reports on these mechanisms in *solid* proteins or cell components. The

‡ Ecole Normale Supérieure de Lyon.
§ Institut de Biologie et Chimie des Protéines.

(1) Halle, B. *Philos. Trans. R. Soc. London Ser. B: Biol. Sci.* **2004,** *359*, 1207−1223.
(2) Otting, G. *Prog. NMR Spectrosc.* **1997,** *31*, 259−285.
(3) van Zijl, P. C.; Zhou, J.; Mori, N.; Payen, J. F.; Wilson, D.; Mori, S. *Magn. Reson. Med.* **2003,** *49*, 440−449.
(4) Modig, K.; Liepinsh, E.; Otting, G.; Halle, B. *J. Am. Chem. Soc.* **2004,** *126*, 102−114.
(5) Halle, B. *J. Chem. Phys.* **2003,** *119*, 12372−12385.
(6) Van deVen, F. J. M.; Janssen, H. G. J.; Gräslund, A.; Hilbers, C. W. *J. Magn. Reson.* **1988,** *79*, 221−235.
(7) Halle, B.; Andersson, T. *J. Am. Chem. Soc.* **1981,** *103*, 500−508.
(8) Liepinsh, E.; Otting, G. *Magn. Reson. Med.* **1996,** *35*, 30−42.

10.1021/ja060866q CCC: $33.50

first studies on solid proteins included hydrogen exchange studies on lysozyme[9,10] and bovine pancreatic trypsin inhibitor (BPTI)[11] crystals, using H/D exchange, followed by quenching and observation of the exchanged sites by subsequent liquid-state NMR studies of the dissolved crystals. These studies revealed exchange rates slower than those in solution for slowly exchanging, buried amide protons. Magnetic relaxation dispersion studies were done on the water molecules in different protein crystals (see Venu et al.[12] and references therein) and were interpreted by different models, but recent work concludes that the observed relaxation dispersion is dominated by a few buried water molecules rather than by the traditional surface hydration previously invoked, and that the contribution from rapidly exchanging protein hydrogens cannot be neglected.[12] Water ^{2}H NMR studies on protein crystals reported deuterium quadrupole splittings of the same order of magnitude in various protein crystals.[12] In contrast, different values for deuterium T_1 relaxation times have been reported for BPTI and lysozyme crystals.[12−14] These differences were attributed to labile protein deuterons, which make a dominant contribution to T_1, mainly at the high pH used in the BPTI study (pH 9.5), but also at the lower pH of the lysozyme crystals (pH 4.5). Only recently, magnetization transfer from double-quantum (DQ) filtered solid-like lattice protons to water protons by chemical exchange has been described as a new source of contrast in imaging.[15]

High-resolution solid-state NMR allows the site-resolved observation of water−protein interactions and, as such, represents a potentially powerful tool to obtain a more detailed picture of hydration in biomolecular solids. Several studies have been performed with this aim on model solid-state protein samples over the past few years. In line with the pioneering work of Harbison and co-workers,[16] we reported recently site-resolved chemical exchange on the millisecond time scale in the microcrystalline protein Crh (catabolite repression histidine-containing phosphocarrier protein).[17,18] In another study, Zilm and co-workers assigned protein−water cross-peaks in microcrystalline ubiquitin to NOE interactions with surface-bound solvent molecules.[19] The most recent study done on microcrystalline SH3 reports the presence of solid-like bound water molecules through the observation of intermolecular dipolar magnetization transfer.[20]

Although we have shown that, for microcrystalline Crh, in conventional heteronuclear correlation (HETCOR) spectra recorded at 5 °C, water−protein cross-peaks originate mainly from chemical exchange between protein side chain labile protons and solvent molecules,[17,18] other mechanisms of interaction cannot be excluded. Figure 1 shows possible intermolecular magnetization transfer schemes between water and the protein.

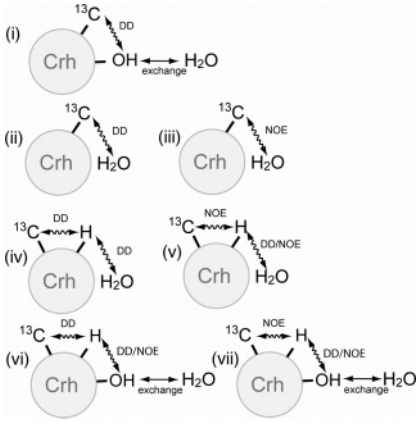

Figure 1. Schematic representation of possible mechanisms for magnetization transfer between water protons and protein carbon-13 atoms. DD stands for direct coherent dipolar interactions; NOE for transfer via the nuclear Overhauser effect. The hydroxyl protons can be replaced by any other fast-exchanging protons, such as NH_3^+.

They include direct or exchange-relayed interactions through coherent dipolar couplings (DD) or NOE interactions with water molecules. The different schemes illustrate well the high complexity of water−protein interactions in solid proteins and give an idea of the confounding effects one pathway can have on the observation of another.

In this study, we investigate possible coherent dipolar or NOE magnetization transfer pathways between water and the microcrystalline Crh protein (schemes (ii) and (iii) in Figure 1). All experiments were done on perdeuterated Crh in order to avoid confusion between water and Hα protons resonating at or near the water frequency. As the possible water−protein magnetization transfer pathways are difficult to distinguish in simple experiments including a proton longitudinal mixing time, we designed experiments that should yield more detailed information. We probe direct magnetization transfers through dipolar couplings using a set of two-dimensional (2D) HETCOR experiments based on dipolar DQ filters. In these experiments, however, no evidence is found for direct intermolecular magnetization transfer through dipolar couplings between water molecules and protein protons during the mixing time of the experiment, precluding the existence of "solid-like" water molecules with long residence times in Crh. Intermolecular NOE cross-relaxation is probed in the heteronuclear case, i.e., from water protons to protein carbon spins, since ^{1}H−^{1}H NOE interactions are difficult to distinguish from proton spin diffusion and chemical exchange. Our experiments do reveal an additional significant enhancement when irradiating at the water proton frequency, but we remark, however, that this can also result partly from exchange-relayed saturation transfers.

2. Materials and Methods

2.1. Sample Preparation. Crh was overexpressed with a C-terminal LQ(6xHis) extension as described previously.[21] ^{2}H-, ^{13}C-, and ^{15}N-enriched Crh was prepared by growing bacteria in >98% ^{2}H,^{13}C,^{15}N-labeled medium (Silantes). The protein was purified on Ni-NTA agarose (Quiagen) columns, followed by anion-exchange chromatography on a Resource Q column.[22] Crh-containing fractions were dialyzed against

(9) Bentley, G.; Delepierre, M.; Dobson, C.; Wedin, R.; Mason, S.; Poulsen, F. *J. Mol. Biol.* **1983,** *170*, 243−247.
(10) Pedersen, T.; Sigurskjold, B.; Andersen, K.; Kjaer, M.; Poulsen, F.; Dobson, C.; Redfield, C. *J. Mol. Biol.* **1991,** *218*, 413−426.
(11) Gallagher, W.; Tao, F.; Woodward, C. *Biochemistry* **1992,** *31*, 4673−4680.
(12) Venu, K.; Svensson, L. A.; Halle, B. *Biophys. J.* **1999,** *77*, 1074−1085.
(13) Usha, M. G.; Wittebort, R. J. *J. Mol. Biol.* **1989,** *208*, 669−678.
(14) Borah, B.; Bryant, R. G. *Biophys. J.* **1982,** *38*, 47−52.
(15) Neufeld, A.; Eliav, U.; Navon, G. *Magn. Reson. Med.* **2003,** *50*, 229−234.
(16) Harbison, G. S.; Roberts, J. E.; Herzfeld, J.; Griffin, R. G. *J. Am. Chem. Soc.* **1988,** *110*, 7221−7223.
(17) Lesage, A.; Böckmann, A. *J. Am. Chem. Soc.* **2003,** *125*, 13336−13337.
(18) Böckmann, A.; Juy, M.; Bettler, E.; Emsley, L.; Galinier, A.; Penin, F.; Lesage, A. *J. Biomol. NMR* **2005,** *32*, 195−207.
(19) Paulson, E. K.; Morcombe, C. R.; Gaponenko, V.; Dancheck, B.; Byrd, R. A.; Zilm, K. W. *J. Am. Chem. Soc.* **2003,** *125*, 14222−14223.
(20) Chevelkov, V.; Faelber, K.; Diehl, A.; Heinemann, U.; Oschkinat, H.; Reif, B. *J. Biomol. NMR* **2005,** *31*, 295−310.
(21) Galinier, A.; Haiech, J.; Kilhoffer, M. C.; Jaquinod, M.; Stulke, J.; Deutscher, J.; Martin-Verstraete, I. *Proc. Natl. Acad. Sci. U.S.A.* **1997,** *94*, 8439−8444.
(22) Penin, F.; Favier, A.; Montserret, R.; Brutscher, B.; Deutscher, J.; Marion, D.; Galinier, A. *J. Mol. Microbiol. Biotechnol.* **2001,** *3*, 429−432.

20 mM NH_4HCO_3. Exchangeable protons were re-exchanged under denaturing conditions (8 M guanidinium chloride). The protein was renatured by 10-fold dilution into 20 mM NH_4HCO_3 buffer and was afterward desalted. The protein was crystallized as described previously[23] in the presence of 20% poly(ethylene glycol) (PEG) 6000 in a crystallization plate over a 2 M NaCl solution. The crystallization solution comprising the protein was at pH 7. The microcrystals resulting from about 8 mg of protein were centrifuged directly into a 4 mm CRAMPS rotor, and the rotor cap was sealed.

2.2. NMR Spectroscopy. NMR experiments were performed on a Bruker AVANCE DSX 500 MHz wide-bore spectrometer, equipped with a double-resonance 4 mm magic angle spinning (MAS) probe. The temperature of the sample was regulated at 267 K, corresponding to an actual sample temperature of about 5−10 °C, depending on the spinning frequency. In all experiments containing a cross-polarization (CP) step, a ramped CP[24,25] was used with radio frequency (rf) fields of 56 and 83 kHz on the carbon and proton channels, respectively. During t_2, the SPINAL-64 sequence[26] was applied at a decoupling power of 66 kHz. Proton and carbon chemical shifts were referenced externally to DSS (2,2-dimethylsilapentane-5-sulfonic acid).[27]

The conventional $^1H-^{13}C$ HETCOR[28] spectra (corresponding to pulse sequences of Figure 2A,B) were obtained at a spinning frequency of 12.5 kHz, while MAS rates of 10 kHz were used for the DQ filtered and edited HETCOR spectra (corresponding to pulse sequences of Figure 2C,D). In the DQ filtered and edited HETCOR experiments, the POST-C7 block[29] was used at a rf field of 70 kHz with excitation and reconversion periods of 200 μs each. A CP contact time of 1 ms has been used in these experiment in order to minimize potential correlations arising from exchange with water during the CP step. Even shorter CP times resulted in important loss in signal/noise. When applied, homonuclear decoupling in t_1 was achieved with the phase-modulated DUMBO-1 scheme[30] at a field of 83 kHz. Pre-pulses of 1.5 μs were used to rotate proton magnetization from the tilted transverse plane under DUMBO-1 decoupling to the (x,y) plane of the laboratory frame and back ($-\theta_1$). As described previously,[31,32] the length and orientation of these short pulses (relative to those of the effective field of the decoupling sequence) were carefully adjusted to minimize quadrature images and zero frequency peaks in ω_1. In all t_1 homonuclear decoupled spectra, proton chemical shifts in the ω_1 dimension were corrected by applying a scaling factor of 0.46, as determined experimentally from a ^1H spectrum of L-alanine.[31] Quadrature detection in ω_1 was achieved using the States[33] and States-TPPI[34] methods for the conventional and DQ HETCOR experiments, respectively.

The 2D $^{13}C-^{13}C$ radio frequency assisted diffusion (RAD)[35] (or dipolar-assisted resonance recoupling, DARR[36]) spectrum was acquired with a proton rf field of 10 kHz during the mixing time. The mixing time was set to 10 ms. Acquisition times of 5.6 and 15 ms were used in the indirect and direct dimensions, respectively. A total of 300 increments were collected, with 128 scans each and a repetition delay of 2 s.

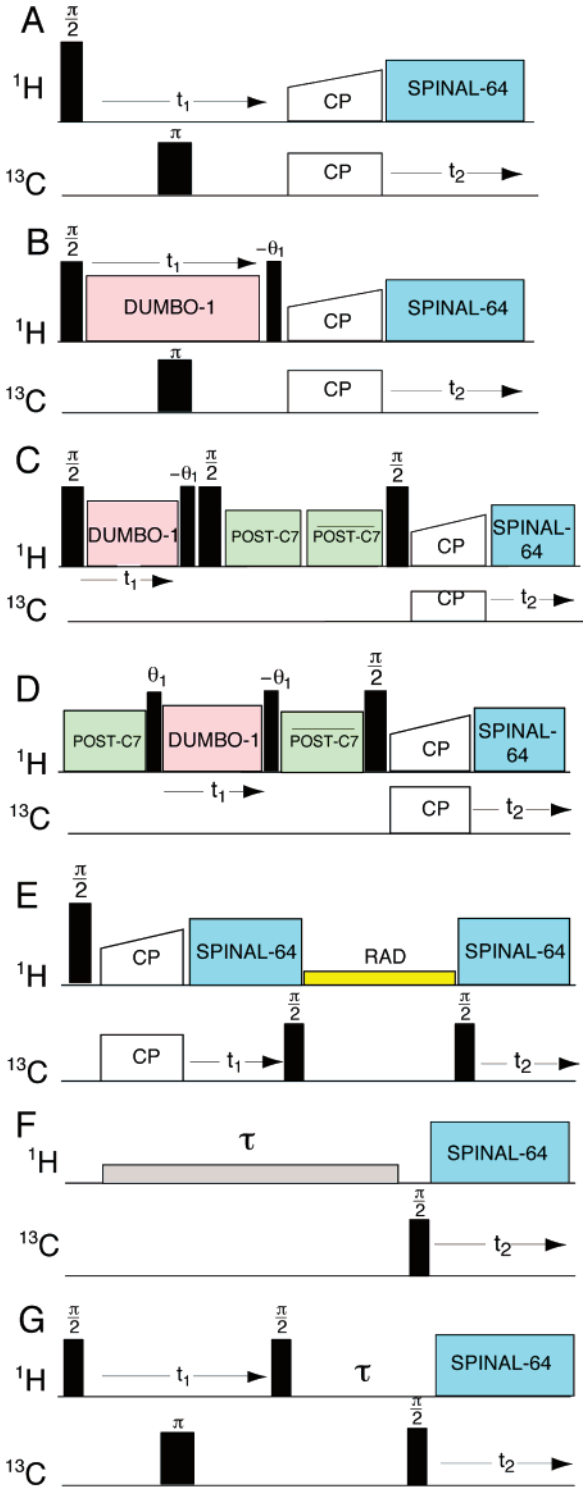

Figure 2. (A,B) Pulse sequences for conventional 2D HETCOR experiments recorded with (A) or without (B) DUMBO-1 homonuclear decoupling during t_1. (C,D) Pulse sequences for double-quantum filtered (C) and double-quantum edited HETCOR experiments (D). The post-C7 block[29] has been used for excitation and reconversion of proton DQ coherences. The 2D RAD[35] (or DARR[36]) $^{13}C-^{13}C$ correlation experiment is shown in (E). (F) Pulse sequence for the 1D heteronuclear NOE experiment. (G) Pulse sequence for the 2D heteronuclear NOE (HOESY) experiment.

(23) Böckmann, A.; Lange, A.; Galinier, A.; Luca, S.; Giraud, N.; Juy, M.; Heise, H.; Montserret, R.; Penin, F.; Baldus, M. *J. Biomol. NMR* **2003,** *27*, 323−339.
(24) Metz, G.; Wu, X. L.; Smith, S. O. *J. Magn. Reson. Ser. A* **1994,** *110*, 219−227.
(25) Hediger, S.; Meier, B. H.; Ernst, R. R. *Chem. Phys. Lett.* **1995,** *240*, 449−456.
(26) Fung, B. M.; Khitrin, A. K.; Ermolaev, K. *J. Magn. Reson.* **2000,** *142*, 97−101.
(27) Markley, J. L.; Bax, A.; Arata, Y.; Hilbers, C. W.; Kaptein, R.; Sykes, B. D.; Wright, P. E.; Wüthrich, K. *Eur. J. Biochem.* **1998,** *256*, 1−15.
(28) van Rossum, B.-J.; Förster, H.; de Groot, H. J. M. *J. Magn. Reson.* **1997,** *124*, 516−519.
(29) Hohwy, M.; Jakobsen, H. J.; Edén, M.; Levitt, M. H.; Nielsen, N. C. *J. Chem. Phys.* **1998,** *108*, 2686−2694.
(30) Sakellariou, D.; Lesage, A.; Hodgkinson, P.; Emsley, L. *Chem. Phys. Lett.* **2000,** *319*, 253−260.
(31) Lesage, A.; Sakellariou, D.; Hediger, S.; Elena, B.; Charmont, P.; Steuernagel, S.; Emsley, L. *J. Magn. Reson.* **2003,** *163*, 105−113.
(32) Brown, S. P.; Lesage, A.; Elena, B.; Emsley, L. *J. Am. Chem. Soc.* **2004,** *126*, 13230−13231.
(33) States, D. J.; Haberkorn, R. A.; Ruben, D. J. *J. Magn. Reson.* **1982,** *48*, 286−292.
(34) Marion, D.; Ikura, M.; Tschudin, R.; Bax, A. *J. Magn. Reson.* **1989,** *85*, 393−399.
(35) Morcombe, C. R.; Gaponenko, V.; Byrd, R. A.; Zilm, K. W. *J. Am. Chem. Soc.* **2004,** *126*, 7196−7197.
(36) Takegoshi, K.; Nakamura, S.; Terao, T. *Chem. Phys. Lett.* **2001,** *344*, 631−637.

Heteronuclear one-dimensional (1D) saturation transfer experiments were performed by applying a long rf irradiation period on protons (typically a few seconds, see figure captions) at a rf power of 0.7 kHz, followed by a ^{13}C 90° detection pulse. The corresponding pulse sequence is shown in Figure 2F. The spinning frequency was 7 kHz, and the repetition delay was adjusted so that its value plus the irradiation time was kept constant at 60 s. The 2D heteronuclear Overhauser enhancement spectroscopy (HOESY) experiment (pulse sequence in Figure 2G) was carried out using the conventional pulse scheme described in the literature.[37] Proton and carbon-13 90° pulses of 2.9 and 3.1 μs, respectively, were used. SPINAL-64 decoupling was applied during direct detection.[26] Quadrature detection in t_1 was achieved using the States method.[33] A total of 32 t_1 increments were recorded with 16 scans each. The recycle delay was set to 15 s.

The pulse programs and phase cycles used here are available upon request from the authors. Fitting of the NOE transfer rates and enhancement factors was done using the Kaleidagraph software.

3. Results and Discussion

3.1. Investigation of Direct Dipolar Contacts with Water Molecules. Potential direct intermolecular magnetization transfer through static dipolar couplings between water protons and carbon or proton spins of the protein (schemes (ii) and (iv) in Figure 1) was investigated using a set of HETCOR experiments which are shown in Figure 2A−D.

Conventional HETCOR Spectroscopy. The first two pulse sequences (Figure 2A,B) correspond to conventional HETCOR experiments, in which proton magnetization evolves during t_1, before being transferred to ^{13}C spins by a CP step, homonuclear decoupling being applied (Figure 2A) or not (Figure 2B) during the indirect evolution time. The resulting spectra recorded on deuterated microcrystalline Crh are shown in Figure 3A,B. Note that, as discussed earlier,[17,18] besides exchangeable protons which were re-exchanged with water, residual protonation is present in this deuterated Crh sample, mainly on methyl groups. In contrast, α-protons, which could interfere with measurements at the water frequency, have been shown to be fully replaced by deuterons.[17,18] In the absence of homonuclear decoupling, the proton line widths of protein resonances are significantly larger than those obtained in the DUMBO-1 decoupled spectrum, indicating that the sample rotation alone (at a spinning frequency of 12.5 kHz) is not sufficient to remove proton−proton dipolar couplings in this deuterated sample. Indeed, proton line widths as narrow as 0.2 ppm are observed in the aliphatic part of the spectrum under DUMBO-1 decoupling. In contrast, some resonances are broadened beyond detection when no decoupling is used (Figure 3A), as is the case for the Thr 12 Hγ1/Cβ cross-peak (at 4.5/73.5 ppm).

Several cross-signals are visible at the water frequency in Figure 3A,B (highlighted in blue) which were previously assigned to water−protein magnetization transfer by chemical exchange via the site-selective identification of the corresponding carbon resonances.[17,18] These signals in the displayed region mainly involve fast-exchanging hydroxyl and NH_3^+ protons (scheme (i) in Figure 1). In the absence of homonuclear decoupling (Figure 3A), these resonances display relatively narrow proton line widths of about 120 Hz. This value indicates that chemical exchange takes place in the fast intermediate exchange regime, since the linewidth lies between that observed for bulk water in a 1D proton spectrum (about 20 Hz) and those

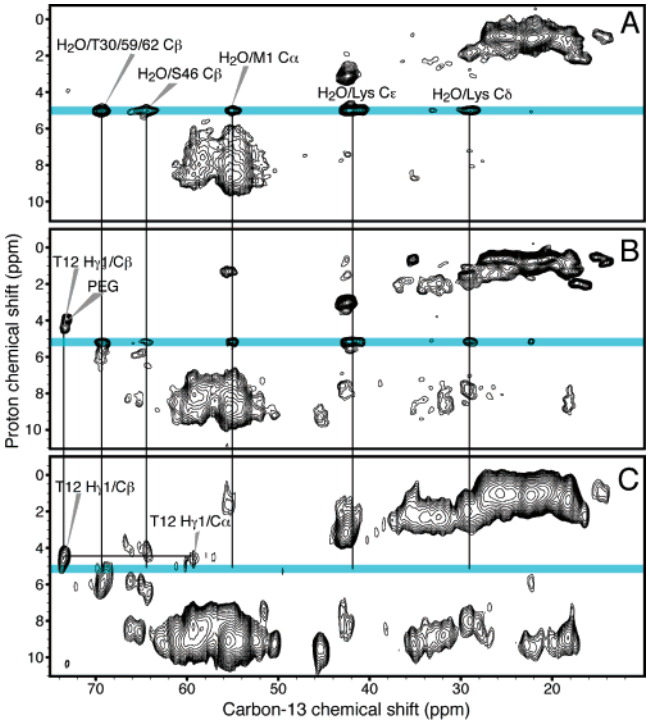

Figure 3. Two-dimensional $^1H-^{13}C$ correlation spectra recorded on microcrystalline deuterated Crh. (A) A conventional HETCOR spectrum acquired with no homonuclear decoupling in t_1 (obtained with the pulse sequence of Figure 2A). A total of 116 t_1 increments with 80 scans each were recorded, with total acquisition times of 8.1 and 10 ms in t_1 and t_2, respectively. (B) A similar HETCOR spectrum acquired with the same acquisition parameters, but with homonuclear proton decoupling in t_1 (obtained with pulse sequence of Figure 2B). A 2 ms contact time was used in the CP step for both spectra, and a carbon π pulse of 7 μs was applied in the middle of the t_1 evolution period.[38] The recyle delay was 3 s. Proton line widths as narrow as 0.2 ppm were obtained in the aliphatic part of the spectrum. (C) A DQ filtered HETCOR spectrum (obtained with the pulse sequence of Figure 2C). A total of 256 t_1 increments with 480 scans each were recorded. The total acquisition times in t_1 and t_2 were 4.1 and 15 ms, respectively.

of the protein proton resonances in the absence of decoupling (typically between 500 and 1000 Hz). As expected, these signals resonate at the water frequency due to fast exchange with a large number of water molecules. Interestingly, in the presence of homonuclear decoupling (Figure 3B), the proton lines at the water frequency are only slightly reduced in the uncorrected spectrum (about 90 Hz). Remarkably, line widths of about 200 Hz are obtained after application of the scaling factor in the ω_1 dimension (see the Experimental Section); i.e., the resonances observed at the water frequency are larger in the presence of homonuclear decoupling. This observation is actually consistent with exchange in the intermediate to fast regime, where the line broadening of the water resonance is a function of the line width of the labile protein proton (reduced with the application of DUMBO-1 decoupling) and the exchange rate (not affected by homonuclear decoupling). However, a quantification of the exchange rates is not possible from these spectra since, in contrast to homonuclear spectra featuring a diagonal signal, in this case we are not able to determine the fraction of water protons in exchange with the protein protons. Thus, besides these exchange cross-peaks, no direct contact corresponding to a static dipolar magnetization transfer from water protons to protein carbon spins is observed at the water frequency in conventional 2D HETCOR spectra as could be potentially expected if tightly

(37) Yu, C.; Levy, G. *J. Am. Chem. Soc.* **1984**, *106*, 3.

bound "solid-like" water molecules were present (scheme (ii)). To more firmly exclude contributions to these signals other than chemical exchange, notably dipolar interactions, we investigate this in the following using DQ filtered and edited spectroscopy.

Double-Quantum HETCOR Spectroscopy. Coherent dipolar-based transfers were further investigated by probing $^1H-^1H$ dipolar contacts between water and protein protons (scheme (iv)). Intermolecular proton−proton contacts with the solvent can indeed be expected to be more sensitive probes of local proximities than proton−carbon contacts, due to larger dipolar couplings and (usually) smaller distances between the nuclei involved. We probe $^1H-^1H$ dipolar contacts between water and protein protons by means of a DQ filter inserted in the HETCOR sequence, as shown in Figure 2C. A POST-C7[29] mixing block is used to create and reconvert proton DQ coherences. This filter selects for pairwise interactions mediated by coherent dipolar couplings. If this type of interaction exists between water and protein protons, intermolecular DQ coherences should be created during the mixing time, and cross-signals would be observed between the proton water frequency in ω_1 and the neighboring carbon of the interacting protein proton in the ω_2 dimension. This would require that a given water proton stays close to a given protein proton for a residence time comparable to the POST-C7 mixing time. The resulting spectrum recorded on deuterated microcyrstalline Crh is shown in Figure 3C.

At the water frequency, the first observation is that nearly all of the cross-signals identified previously by us to have their origin in chemical exchange between water and labile protein protons[17,18] disappear. Thus, the cross-signals involving lysine Cϵ and Cδ carbons are no longer observed, as is also the case for the N-terminal Met 1 Cα. The cross-peak involving Ser 46 Cβ is clearly missing as well. In other words, the magnetization transfer corresponding to the pathway of scheme (vi) in Figure 1, i.e., t_1 evolution at the water frequency of a labile proton, creation of DQ coherences with an adjacent protein proton by dipolar coupling, reconversion, and detection on the neighboring carbon-13 spin, is quenched in this experiment. This implies that the dipolar couplings involving the exchanging protons are inefficient due to fast exchange rates (corresponding to residence times shorter than the millisecond time scale) and do not allow for creation of pairwise DQ and reconversion during the mixing periods. The second observation is that, in the DQ filtered spectrum of Figure 3C, no new cross-peaks are observed at the water frequency that would originate from coherent dipolar-mediated intermolecular transfer with the solvent (scheme (ii)).

Although no signals are observed any more precisely at the water frequency, some intensity can still be detected near the water frequency for carbon chemical shifts of 73.5 and 69 ppm (corresponding respectively to T12 and T57 Cβ resonances), as shown in the expansion of the DQ filtered HETCOR spectrum in Figure 4A. As the hydroxyl protons of Thr 12 and Thr 57 form hydrogen bonds to two highly conserved water molecules in the Crh crystal structure, we investigate the origin of the corresponding cross-peaks in more detail in the following.

T12 and T57 Correlations at the Water Frequency. The correlations observed near the water frequency in the DQ HETCOR spectrum with Thr 12 and Thr 57 Cβ resonances can potentially correspond to a magnetization transfer from water protons; however, they much more likely correspond to their hydroxyl protons, which have been shown, for both residues, to be slowly exchangeable protons (with respect to the millisecond time scale).[18] Indeed, in the DQ filtered spectrum, we actually observe very clearly all hydroxyl protons previously identified to show slow exchange with solvent protons on the observed time scale. Thus, as shown in Figure 4A, one can unequivocally assign, in addition to the Thr 12 Hγ proton, by comparison between this DQ filtered spectrum and a 2D RAD spectrum (Figure 4C), Ser 31, Ser 56, Ser 52, and Thr 57 hydroxyl protons. The signal intensity observed near the water resonance at the Thr 12 Cβ chemical shift is probably due to proton line broadening observed in the DQ filtered spectrum (due to a shorter t_1 indirect detection time). This is supported by the Thr 12 Hγ1/Cα cross-signal at 4.5/59 ppm (not observed in conventional HETCOR spectra), which likely corresponds to the creation of a Thr 12 Hγ1/HN DQ coherence during the mixing time, and which resonates at higher field than the water protons.

Although Thr 12 and Thr 57 Hγ1 resonate near the water frequency, the peak intensity detected at the water frequency could still indicate a DQ interaction between the slowly exchanging hydroxyl protons and water protons. Indeed, as shown in Figure 4, Thr 12 and Thr 57 are direct neighbors to two highly conserved water molecules, W 19 and W 24, respectively. These two water molecules seem to be essential to dimer stabilization by bridging Thr 12 from chain A to Thr 57 from chain B, via (Tyr 12 N−H)···HOH···(HO−Cβ Tyr 57) intermolecular hydrogen bonds. These water molecules have been observed within 0.15 Å in both crystal structures of Crh solved so far (at room temperature, PDB code 1mu4,[39] and at cryogenic temperature, PDB code 1mo1 (Se-Met Crh, M. Juy, personal communication)). To check whether a coherent dipolar interaction can be detected with these two key water molecules, we used an experiment with a DQ evolution in t_1 in order to elucidate unambiguously the chemical shifts of the proton pairs at the origin of the two cross-signals resonating around 5 ppm in the DQ filtered experiment. Figure 2D shows the pulse sequence of the corresponding experiment in which an indirect proton evolution time of DQ coherences is bracketed between a C7-type[40] excitation and reconversion period.[32] An extract of the resulting ^1H DQ and ^{13}C detected HETCOR spectrum is shown in Figure 4B. It features, within the range of the ω_2 Cα frequency (50−66 ppm), NH−NH DQ cross-signals in the ω_1 dimension around 18 ppm, NH−methyl proton cross-signals around 11 ppm, and a few methyl signals around 4 ppm, mostly from alanines. The cross-signals of interest are those that originate from the interactions involving the hydroxyl protons of Thr 12 and Thr 57, at the carbon chemical shifts of 73.5 and 69 ppm. The chemical shifts of these DQ signals are observed respectively at 12.3/73.5 and 13.1/69 ppm in the ω_2/ω_1 dimensions. These correlations thus belong to pairs of hydroxyl and amide protons, as indicated by the chemical shift of the second DQ partner of 7.9 and 7.6 ppm for Thr 12 and Thr 57, respectively. No cross-signals around 10 ppm, which would be indicative of water/hydroxyl proton pairs, were observed in the proton DQ dimension for Thr 12 and Thr 57. We also note here that, for the serine residues, the cross-peaks involving the

(38) Lesage, A.; Emsley, L. *J. Magn. Reson.* **2001,** *148*, 449.
(39) Juy, M.; Penin, F.; Favier, A.; Galinier, A.; Montserret, R.; Haser, R.; Deutscher, J.; Böckmann, A. *J. Mol. Biol.* **2003,** *332*, 767−776.
(40) Feng, X.; Edén, M.; Brinkmann, A.; Luthman, H.; Eriksson, L.; Gräslund, A.; Antzutkin, O. N.; Levitt, M. *J. Am. Chem. Soc.* **1997,** *119*, 12006−12007.

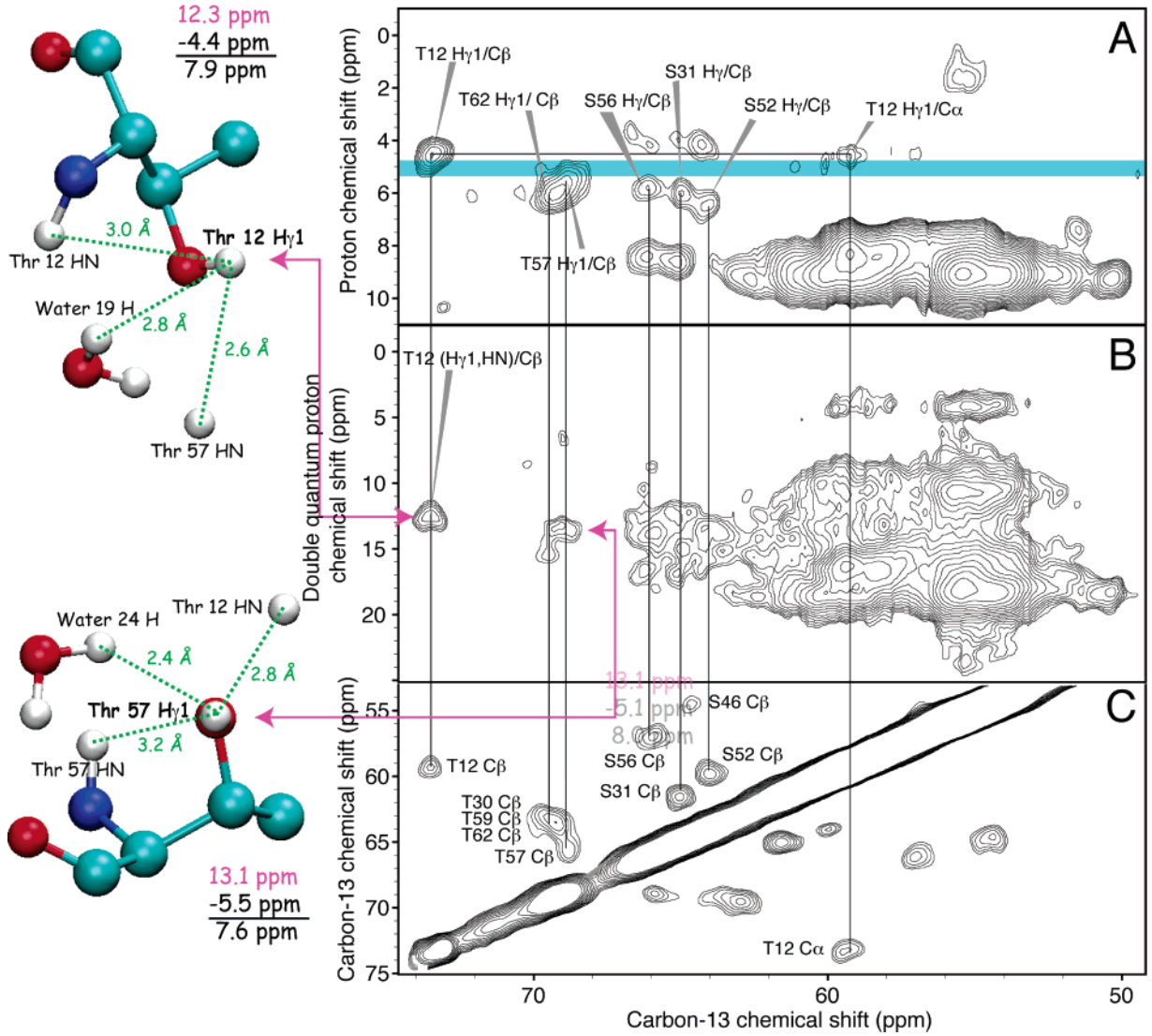

Figure 4. (A) Expansion of the 2D DQ filtered $^{1}H-^{13}C$ HETCOR spectrum recorded using the pulse sequence in Figure 2C, in comparison with (B) a 2D $^{1}H-^{13}C$ DQ edited spectrum recorded using the pulse sequence in Figure 2D and (C) a 2D $^{13}C-^{13}C$ RAD correlation spectrum recorded using the pulse sequence in Figure 2E. On the left are shown the nearest neighboring protons of the Hγ1 proton of Thr 12 and Thr 57 residues, including water molecules 19 and 24 as observed in the X-ray structure (PDB code 1mu4[39]).

hydroxyl protons are located in the DQ edited spectrum in the resonance group centered around 14 ppm in the DQ dimension, indicating that these serine hydroxyl protons also create DQ coherences with neighboring amide protons.

The nearest neighboring protons in the crystal structure of hydroxyl Hγ1 protons of Thr 12 and Thr 57 residues are shown in Figure 4 (left), together with the corresponding distances. In both cases, water protons are in very close contact. Despite these short distances between the highly conserved neighboring water molecules and the hydroxyl protons, the fact that no cross-signals can be observed in the DQ edited spectrum indicates that, as mentioned previously, the residence times of these water molecules are shorter than the time necessary to efficiently create and reconvert DQ interactions. This is also in agreement with results from MRD studies in BPTI crystals, which revealed residence times on the microsecond time scale for a small number of water molecules and *subnanosecond* residence times for most of the water molecules.[2,4,12] Longer residence times up to the millisecond time scale were observed only for water molecules completely buried in cavities, such as W 122 in BPTI. Note that, although the two highly conserved water molecules W 19 and W 24 are involved in an extensive hydrogen-bonding network at the dimer interface, they are not buried inside a cavity and are readily solvent accessible.

Internal Water Molecules. Interestingly, in the Crh domain swapped dimer crystal structure (PDB code 1mu4[39]), two internal water molecules are observed, each of them creating hydrogen bonds with Leu 14 NH, Leu 50 CO, and Leu 53 CO from one monomer. For these water molecules, the nearest neighboring amide protons (with internuclear distances shorter than 3 Å) are Leu 14 NH and Leu 53 NH. However, under the experimental conditions used for the DQ HETCOR experiment reported here (Figure 3C), we could not observe any cross-signals between the protons of these buried water molecules and the adjacent nuclei, i.e., Leu 14 Cα and Leu 53 Cα. Again, this indicates that the residence times of even these water molecules, under the conditions used here, are shorter than required for efficient DQ coherence creation. In the same way, these water molecules do not give rise to any CP signal with nearby carbons of less than 3 Å (Leu 50 and Leu 53 C′ at 2.77

and 2.76 Å, respectively), as no signals are observed in the carbonyl backbone region of the HETCOR spectra (data not shown). Note that these water molecules are also conserved in the X-ray structure of selenomethylated Crh (pdb code 1mo1). In addition to the two internal water molecules, several surface water molecules are also found in more or less solvent accessible cavities in the Crh crystal but could not be detected by the DQ filtered experiments.

With regard to the investigation of direct dipolar contacts between solvent and protein protons, we can conclude that, in the DQ experiments used here, no water molecules, even those located in strategic locations important for the protein structure or those found in the interior of the protein, give rise to DQ signals with protein protons, and thus they cannot be regarded as "solid-like" in the same manner as protein protons. Our results indicate that the residence times of the water molecules are shorter than the DQ creation and reconversion times (a few hundreds of microseconds), which is in line with results from MRD data obtained in ubiquitin and BPTI.[12]

3.2. Water−Protein Magnetization Transfer by NOE. Intermolecular NOE is another possible route for magnetization transfer from the solvent (scheme (iii)) and, as such, has already been proposed to explain water−protein interactions observed in the solid state.[19] The following section concerns the investigation of such effects in the microcrystalline protein Crh. As ^{1}H−^{1}H homonuclear NOE is difficult to distinguish from chemical exchange and ^{1}H−^{1}H spin diffusion in solids, we chose to probe potential heteronuclear ^{1}H−^{13}C cross-relaxation between water protons and protein carbon spins (since neither chemical exchange nor spin diffusion can lead to heteronuclear polarization transfer). Heteronuclear NOE in high-resolution solid-state NMR was described in the 1980s by Naito et al.[41,42] on the model sample L-alanine, and more recently by Terao and co-workers[43,44] for small molecules as well as for lyophilized proteins. In these latest studies, the heteronuclear magnetization transfers were investigated using the nuclear Overhauser polarization (NOP) technique, which is based on proton irradiation under DARR[36] conditions. These transfers have been shown to proceed mainly from methyl groups, the enhancement being then redistributed by spin diffusion to all the ^{13}C spins. Enhancement factors close to 2 have been reported using the NOP scheme, and at the extreme narrowing limit the maximum enhancement reaches a factor of 3. In the present work, proton irradiation was applied at off-DARR conditions ($\omega_1 \neq \omega_r$) in order to observe more selective transfers. The kinetics and dependence on the irradiation frequency of the heteronuclear NOE enhancement were first probed on the model sample L-alanine. We then investigated these features on protonated and deuterated microcrystalline Crh, with the intention of analyzing the experimental data in the context of water−protein magnetization transfer by NOE in a solid model protein.

Model Sample L-Alanine. Figure 5A shows in red the spectra for fully ^{13}C-labeled (top) and natural abundance (bottom) L-alanine recorded with the pulse sequence shown in Figure 2F, consisting of a long rf irradiation period on protons (typically several seconds) followed by a 90° carbon read pulse. For comparison are shown in black the corresponding spectra without proton irradiation prior to the 90° carbon read pulse (shifted to the right for better visibility). In the following, the NOE enhancement is defined as I_z/I_z^0, where I_z and I_z^0 are respectively the observed intensities in experiments with and without saturation. At natural abundance, for a proton irradiation time of 4 s, we see mainly a signal enhancement by NOE on the methyl carbon. In contrast, for fully ^{13}C-labeled L-alanine, we clearly observe an enhancement for all three carbon resonances. In light of the recent work of Takegoshi et al., these results can be interpreted on the basis of polarization enhancement of the methyl carbons by NOE from their attached fast-rotating protons, followed by redistribution to the other carbon-13 spins by homonuclear spin diffusion. In other words, at a spinning frequency of 7 kHz, even at off-DARR conditions, the spin diffusion among the carbon spins that occurs during the irradiation period appears to be efficient enough to redistribute the enhanced methyl carbon polarization, leading to a uniform NOE enhancement. At natural abundance, the Cα and CO spins are only insignificantly enhanced by direct transfer from the methyl protons, as also shown by Takegoshi et al. in nonlabeled dimedone.[43]

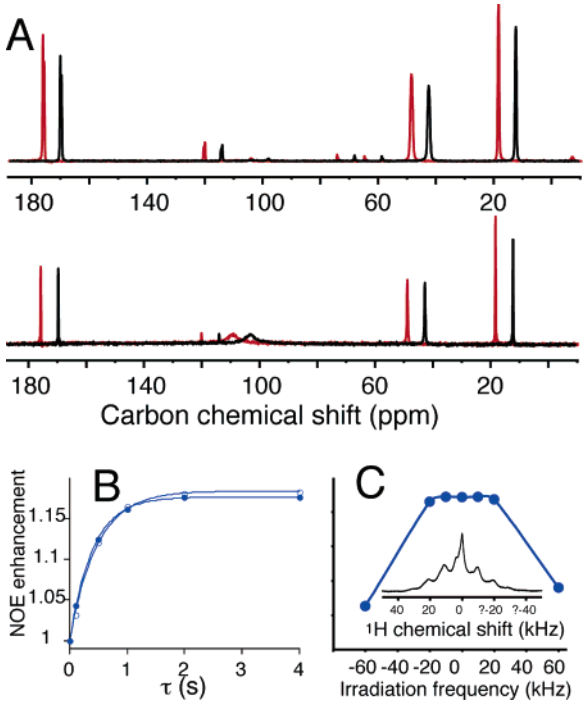

Figure 5. (A) One-dimensional carbon-13 spectrum of fully ^{13}C-labeled (top) and natural abundance (bottom) L-alanine recorded with (in red) and without (in black, right-shifted) proton irradiation prior to the 90° carbon read pulse. A total of 64 scans were recorded with a relaxation interval of 60 s. For the saturation experiments, a proton irradiation time of 4 s was used. (B) Time dependence of the NOE enhancement on the methyl carbon in fully ^{13}C-labeled (filled circles) and natural abundance (open circles) L-alanine. (C) Offset dependence of the NOE enhancement on the methyl carbon in fully ^{13}C-labeled L-alanine. The corresponding MAS proton spectrum is shown in the inset. All the experiments were done at a spinning frequency of 7 kHz.

The observed signal intensity buildups for the methyl carbons are shown in Figure 5B for both the natural abundance and fully ^{13}C-labeled samples. The curves were fitted to the following single-exponential function:

(41) Naito, A.; Ganapathy, S.; Akasaka, K.; McDowell, C. A. *J. Magn. Reson.* **1983,** *54*, 226.
(42) Naito, A.; McDowell, C. A. *J. Chem. Phys.* **1986,** *84*, 4181.
(43) Takegoshi, K.; Terao, T. *J. Chem. Phys.* **2002,** *117*, 1700−1707.
(44) Katoh, E.; Takegoshi, K.; Terao, T. *J. Am. Chem. Soc.* **2004**, *126*, 3653−3657.

$$I_z(t)/I_z^0 = \eta_{NOE}(1 - \exp(-k_{NOE}t)) + 1$$

using the enhancement factor η_{NOE} and k_{NOE}, the rate constant, as fitting parameters.[44] Enhancement factors of 0.18 are observed for the methyl carbon in both samples, with a slightly faster rate k_{NOE} for ^{13}C-labeled L-alanine (2.5 s^{-1}, versus 2.1 s^{-1} in the natural abundance sample). As illustrated for the fully ^{13}C-labeled sample (Figure 5C), the NOE enhancement shows very little dependence on the proton irradiation frequency. This is expected in the case of a strongly dipolar coupled proton bath, which leads to a homogeneously broadened proton spectrum, as is the case for the model sample L-alanine (see proton spectrum in the inset of Figure 5C).

NOE Enhancements in Microcrystalline Crh. Figure 6A shows a comparison of a carbon-13 spectrum of protonated microcrystalline Crh recorded with the pulse sequence of Figure 2F with (top spectrum) and without (bottom spectrum) proton irradiation. Figure 6B shows the magnetization buildup for two different resonances in protonated (^{1}H) and deuterated (^{2}H) Crh, namely a methyl carbon (at 17.6 ppm) and a carbonyl carbon (at 175.5 ppm). These curves were fitted according to the single-exponential function used previously for L-alanine, and the resulting values for η_{NOE} and k_{NOE} are shown in Table 1 (fitted parameters are also reported in Table 1 for a resonance representative of the Cα region, chosen at 52 ppm).

As for the case of L-alanine, the enhancement factors are very similar for all the carbon resonances, reflecting the efficient redistribution of the magnetization by carbon-13 spin diffusion after site-specific polarization enhancement by NOE from the mobile protonated groups, namely CH_3 groups. The initial rates are, however, quite different, likely due to differences in T_1 longitudinal relaxation times for the different carbon spins. As expected, smaller enhancements are observed for deuterated Crh, due to the presence of less protonated methyl groups. Although the major contribution to the NOE enhancements seems to originate from the methyl groups, we are aware that, in proteins, it is possible that side-chain mobility from other groups can contribute as well, as already pointed out by Takegoshi et al.[43]

Figure 7 shows the NOE enhancements in protonated and deuterated Crh as a function of the proton irradiation frequency. The MAS 1D proton spectrum is shown above to indicate the position of water and PEG resonances. Although the proton offset profile of the NOE enhancement is less flat than the one reported for L-alanine (Figure 5), we still observe significant enhancements over a frequency range of 60 kHz, reflecting again the homogeneous nature of the protein proton spectrum. As expected, for the deuterated protein, the frequency range over which NOE enhancements can be detected is narrower, indicating the relative breaking up of the proton bath by the reduced proton density. For comparison, the offset dependence of the NOE enhancement observed for the PEG resonance is also shown in Figure 7. The corresponding profile, which displays a strongly marked maximum upon irradiation at the PEG proton frequency, is extremely narrow, indicative of a highly mobile component. No enhancement from solid protons is observed for PEG. More interesting is the observation that, in both the deuterated and protonated samples, the maximum enhancement is observed at the water frequency. This is especially visible for the deuterated sample, for which an enhancement of 1.44 is observed for the resonance representative of methyl carbons

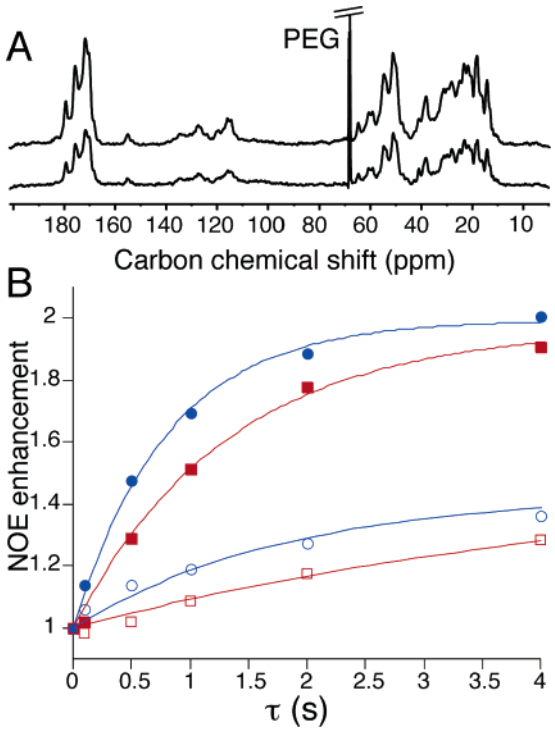

Figure 6. (A) Single-pulse carbon-13 spectra of protonated Crh recorded with (top) and without (bottom) proton irradiation prior to the 90° read pulse. The number of scans was 64 and the repetition delay 40 s. An irradiation period of 4 s was used for the top spectrum. The proton irradiation frequency was set off water resonance at 12 ppm. (B) Experimentally observed NOE enhancements for resonances representative of methyl (blue circles) and carbonyl (red squares) carbons (at 17.6 and 175.5 ppm, respectively) in protonated (filled symbols) and deuterated (open symbols) Crh.

Table 1. Best-Fit Parameters for the Time Dependence of the NOE Enhancement in Protonated (p) and Deuterated (d) Crh[a]

	η_{NOE}	k_{NOE} (s^{-1})
CH_3 (p)	0.99 ± 0.02	1.23 ± 0.08
Cα (p)	0.93 ± 0.05	0.81 ± 0.10
CO (p)	0.97 ± 0.04	0.75 ± 0.07
CH_3 (d)	0.48 ± 0.02	0.49 ± 0.06
Cα (d)	0.46 ± 0.04	0.20 ± 0.03
CO (d)	0.48 ± 0.03	0.21 ± 0.03

[a] η_{NOE} and k_{NOE} represent respectively the NOE enhancement factor and the rate constant. Proton irradiation was done off water resonance.

when irradiating at the solvent frequency, versus 1.37 upon irradiation at the methyl proton frequency, which corresponds to an increase in the fractional NOE enhancement of about 19%.

Kinetics of NOE on Microcrystalline Crh. Figure 8 shows the time dependencies of peak intensities of Crh resonances representative of methyl (blue), carbonyl (red), and Cα (gray) carbons. The data were fitted to a single-exponential function (see above) to obtain the values for the NOE enhancement factor, η_{NOE}, and the rate, k_{NOE}, as reported in Table 2. As indicated previously, the observed maximum enhancement η_{NOE} is significantly larger for irradiation at the water resonance. The buildup rates k_{NOE} are, however, equivalent within the error bars for off- or on-water-resonance irradiation for all carbon resonances considered. Note here that the single-exponential fitting does not reproduce the data well, particularly in the initial NOE buildup region, shown in the expansion of Figure 8B. As pointed out by Terao and co-workers,[44] the equation used for the fitting procedure (see above) is indeed derived at the slow ^{13}C−^{13}C

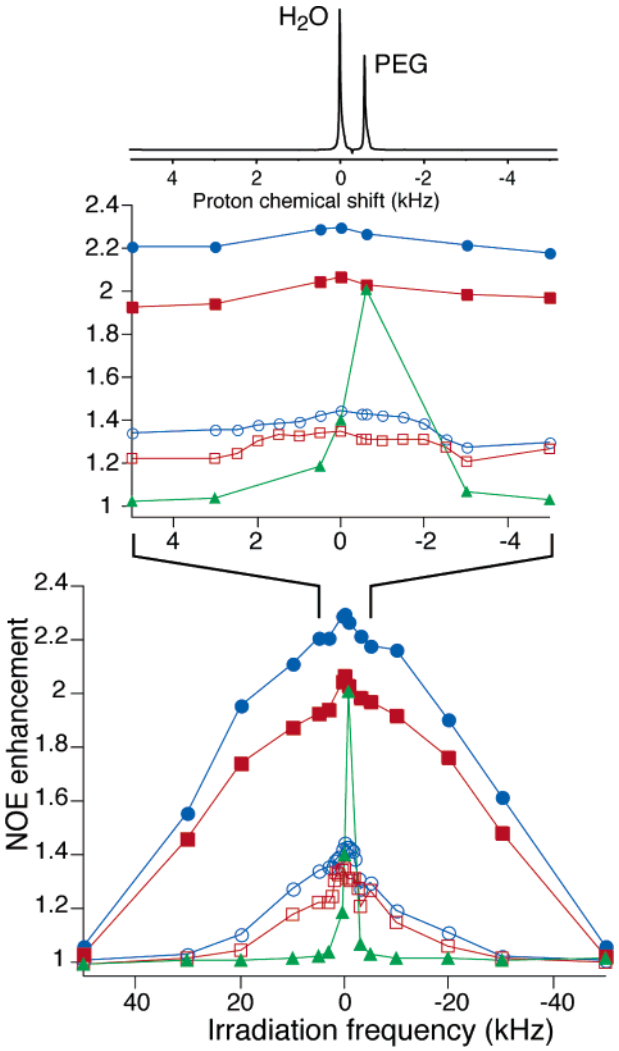

Figure 7. Offset dependence of NOE enhancements in protonated (filled symbols) and deuterated (open symbols) Crh. These dependencies are shown for resonances representative of both methyl (blue circles) and carbonyl spins (red sqaures) (at 17 and 172 ppm, respectively). The irradiation time was set to 4 s, and a total of 64 scans were recorded. The NOE enhancement observed for the carbon peak of PEG is also shown in green triangles.

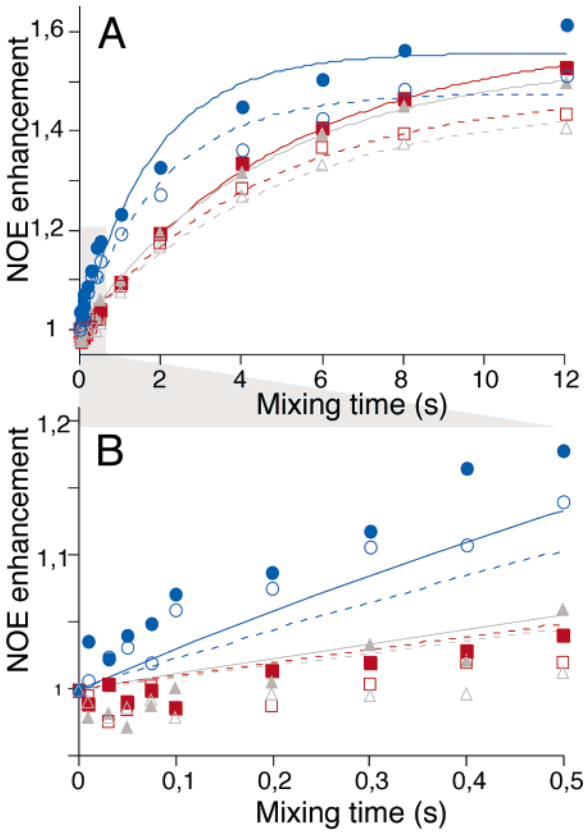

Figure 8. (A) NOE buildup of methyl (blue circles), carbonyl (red squares), and Cα (gray triangles) resonances and in deuterated Crh when irradiating at the water frequency (filled symbols) and off the water resonance (open symbols). (B) The extract of the first 0.5 ms of the data. The lines are the best-fit curves for on-water-resonance (solid) and off-water-resonance (dashed) irradiation, with the best-fit parameters collated in Table 2.

Table 2. Best-Fit Parameters for On-Water-Resonance Irradiation on Deuterated Crh of the Enhancement Factor, η_{NOE}, and the NOE Rate Constant, k_{NOE}

	η_{NOE}	k_{NOE} (s^{-1})
CH_3	0.56 ± 0.02	0.55 ± 0.08
Cα	0.54 ± 0.02	0.21 ± 0.02
CO	0.59 ± 0.02	0.19 ± 0.02

polarization transfer limit and thus underestimates NOE enhancements on the methyl groups while overestimating NOEs for the remaining carbons in the initial rate.

Nevertheless, the observed delayed buildup of the backbone resonances, whether on-water-resonance or off-water-resonance irradiation is used, clearly indicates that the major part of the magnetization is still transferred in both cases via the methyl protons to the methyl carbons, followed by redistribution to the remaining carbon atoms. In other words, upon irradiation on or off water resonance, carbonyl carbons, as well as Cα carbons, start gaining magnetization only when methyl carbons start to lose it. Substantial water−protein NOE could be expected to be visible as an additional enhancement on these backbone carbons, even more than on the methyl carbons, which are generally hidden in the inside of the protein. If, however, a NOE induced by the water molecules is relatively weak, the indirect $^{13}C-^{13}C$ magnetization transfer from the methyl carbons will dominate and make it difficult to observe the direct transfer. Under our experimental conditions, the weak signal-to-noise ratio, mainly in the initial region, does not allow for the detection of such small effects, and it is thus difficult to clearly establish the presence of direct intermolecular heteronuclear NOE transfers from water at this stage.

Moreover, although direct water-to-protein NOE is a reasonable mechanism for transfer in this experiment, we cannot, in fact, exclude that the increase in the enhancement observed upon irradiation at the water frequency originates in part from exchangeable protein protons resonating at that frequency. In addition, and perhaps more importantly, more complex relayed mechanisms mediated by chemical exchange and dipolar interactions from water to methyl protons are other possible routes for NOE-type transfers (schemes (v) and (vii) in Figure 1, where in (v) and (vii) the protein proton represents a methyl proton or another highly mobile protein proton). For example, water-to-protein proton magnetization transfer could occur by chemical exchange to a mobile protein proton. This step could then be followed by NOE from this mobile group to the carbons. It could alternatively be followed by spin diffusion among the protons to a methyl group and then transfer via NOE to the carbon spins. Signal from these pathways could be enhanced by irradiating the water resonance, because that would then lead

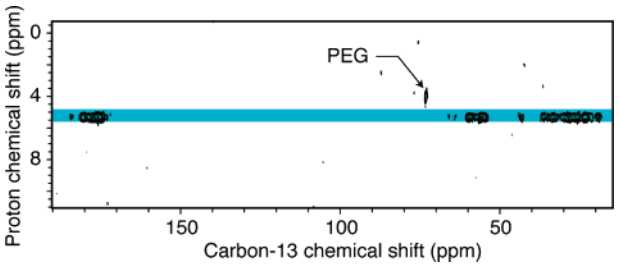

Figure 9. Two-dimensional HOESY spectrum recorded on microcrystalline protonated Crh, with a mixing time τ of 700 ms.

to saturation transfer from the water to the protein protons by chemical exchange (and eventually subsequent spin diffusion). As shown in Figure 9, a 2D HOESY spectrum (recorded with a mixing time of 700 ms) shows cross-signals in the ω_1 dimension at the water frequency alone (with an exception for the PEG resonance) and with all protein carbon resonances and does not allow for the observation of selective direct NOE transfer from water protons. Further investigations, mainly at lower temperatures, where chemical exchange is sufficiently slowed, will have to be conducted to unambiguously determine the role of NOE in these experiments, since they should allow us to separate direct NOE from chemical exchange relayed contributions and thus to more clearly establish the origins of the magnetization transfers by NOE observed in the experiments reported here.

4. Conclusion

In the present study, we have shown that further understanding of water−protein magnetization transfer can be gained using experiments designed to detect specific transfer pathways. Double-quantum filtered or edited HETCOR experiments did not reveal "solid-like" water molecules in Crh, in contrast to results described for the SH3 protein.[20] This allowed us to deduce residence times for surface and internal water molecules shorter than a few hundred microseconds in Crh protein crystals.

Heteronuclear NOE in Crh was also investigated, and buildup rates were analyzed to obtain information on magnetization transfer pathways. We observed that additional enhancements are detected in heteronuclear NOE experiments when irradiating the water resonance. It is, however, difficult to draw a conclusion on the nature of these enhancements, which can be assigned to either direct water−protein NOE between solvent protons and protein carbons or relayed magnetization transfers via chemical exchange from water to protein protons, followed by redistribution of the magnetization by spin diffusion to methyl protons. Further experiments conducted at variable spinning speeds and temperatures should help to establish which mechanism dominates and are currently under investigation in our laboratory.

The investigation of water−protein interactions will certainly be extended to many more proteins in the near future, as deuterated samples become more common and more proteins are being assigned by solid-state NMR. Water−protein interactions will certainly be dependent on the physicochemical conditions of the sample, for example the pH and crystal packing. Studies over wider temperature and pH ranges, as well as studies of the same proteins by other techniques, such as magnetic relaxation dispersion,[1] should help to complete the emerging site-resolved picture of water−protein interactions in solid proteins revealed by high-resolution solid-state NMR. Our work illustrates the high potential of this technique to study hydration in immobilized proteins, which include also membrane proteins and protein fibrils. Finally, the physical properties of water in protein crystals as studied here are of interest not only inasmuch as they relate to protein hydration under physiological solution conditions, but also in connection with relaxation-based contrast in magnetic resonance imaging.[3, 15]

Acknowledgment. The authors acknowledge stimulating discussions with G. Pintacuda and K. W. Zilm. This work was funded by CNRS and the French research ministry (ACI Biologie Cellulaire Moléculaire et Structurale 2003; ANR Jeunes Chercheuses, Jeunes Chercheurs 2005).

JA060866Q